Eur. J. Biochem. **267**, 5093–5100 (2000) © FEBS 2000

Roles of cysteines in rat dipeptidyl peptidase IV/CD26 in processing and proteolytic activity

Jörg Dobers, Sabine Grams, Werner Reutter and Hua Fan

Institut für Molekularbiologie und Biochemie, Freie Universität Berlin, Germany

The multifunctional type II transmembrane glycoprotein, dipeptidyl peptidase IV (DPPIV, EC 3.4.14.5), is expressed by almost all mammalian cells and is identical to the adenosine deaminase binding protein CD26 on lymphocytes. The extracellular part of rat DPPIV can be divided into three domains the middle part of which harbors 10 of the 12 highly conserved cysteine residues. The cysteine-rich domain is responsible for DPPIV-binding to collagen I and to extracellular ADA. The participation of distinct cysteines in disulfide bridges is not yet known. Titration experiments have shown the presence of six free cysteines and three disulfide bridges in native rat DPPIV. To investigate the role of distinct cysteines in the structure–function relationships of rat DPPIV we constructed 12 different cysteine point mutations (C299, C326, C383, C455, C650 mutated to G; C337, C395, C445, C448, C473, C552, C763 mutated to S). Intracellular translocation to the cell surface of stable transfected Chinese hamster ovary cells was examined with antibodies against different epitopes of DPPIV. Surface expression of mutants C326G, C445S and C448S is inhibited totally; mutants C337S, C455G, C473S and C552S show weak expression only. In parallel, the half-life of these mutants is reduced to $< 10\%$ compared with wild-type enzyme. We were able to show that the specific peptidase activity of the mutant protein depends on cell-surface expression, dimerization and the existence of a 150-kDa form demonstrable by nondenaturing SDS/PAGE. We conclude that cysteine residues 326, 337, 445, 448, 455, 473 and 552 in rat DPPIV are essential for the correct folding and intracellular trafficking of this glycoprotein, and therefore for its normal biological properties.

Keywords: CD26; dipeptidyl peptidase IV; disulfide bridge; structure–function relationship.

The multifunctional type II transmembrane glycoprotein, dipeptidyl peptidase IV (DPPIV, EC 3.4.14.5), is expressed by almost all mammalian cells. First described as glycyl-prolyl-naphthylamidase by Hopsu-Havu and colleagues from rat liver [1,2], it is found in a wide range of organs and tissues. Furthermore, DPPIV has been shown to be a activation marker on lymphocytes [3–5]. Soluble forms exist, for example, in lysosomes, human serum [6,7] and *Xenopus laevis* [8].

The membrane-bound wild-type rat enzyme is expressed as a noncovalently linked 210-kDa homodimer at the cell-surface [9]. Whether dimerization occurs prior to Golgi import [10] or after hybrid and complex glycosylation in the late Golgi apparatus [11] is still not known. Rat-DPPIV (767 amino acids) consists of a short cytoplasmic domain, followed by a hydrophobic transmembrane domain of 22 amino acids and an extracellular sequence of 739 amino acids [12]. The sequences of the 110-kDa glycoprotein from rat and the corresponding human and mouse peptidases exhibit very high similarities [13,14]. The primary structure contains eight potential N-glycosylation sites proximate to the transmembrane domain; O-glycosylation has not been detected. The formation of complex N-glycans plays an important role in the stability and function of DPPIV [15].

The glycan-rich domain is followed by a cysteine-rich region containing 10 of the 12 cysteine residues. The active site is located at the C-terminus with the catalytic triad Ser631, Asp709 and His741 [16].

In addition to its well known exopeptidase activity, DPPIV also exhibits endopeptidase activity toward denatured collagen [17]. Its very distinct substrate specifity is important for the processing and modulation of defined peptides and chemokines [5,18]. Knowledge about *in vivo* substrates is still very limited.

As an activation marker, DPPIV/CD26 is expressed at the surface of human lymphocytes, preferentially on $CD4^+$ subsets of T cells, on B cells, macrophages and other immune cells [19]. DPPIV/CD26 harbors important costimulatory functions during T-cell activation and proliferation. Concerning the activation pathway, interaction of the extracellular domain of DPPIV with protein-tyrosine-phosphatase CD45 is essential. The specific interaction of extracellular adenosine deaminase (ADA) with CD26 has been shown to support T-cell proliferation in humans [3]. The ADA-binding domain is located within the cysteine-rich domain. Interestingly, no binding of human ADA could be detected with highly conserved rat/mouse

Correspondence to H. Fan, Institut für Molekularbiologie und Biochemie, Freie Universität Berlin, Arnimallee 22, 14195 Berlin-Dahlem, Germany.
Fax: + 49 308 445 1541, Tel.: + 49 308 445 1544,
E-mail: fanzheng@zedat.fu-berlin.de

Abbreviations: ADA, adenosine deaminase; CAM, cell adhesion molecules; CHO, Chinese hamster ovary; DSS, disuccinimidylsuberate; ER, endoplasmic reticulum; FACS, fluorescence activated cell sorting; FAP, fibroblast activating protein; FITC, fluorescein isothiocyanate; mAb, monoclonal antibody; MEM, modified Eagle's medium; Nbs_2, 5,5′-dithiobis(2-nitrobenzoic acid).

Enzymes: rat DPPIV, dipeptidyl peptidase IV (SWISS-PROT accession no. 118905, EC 3.4.14.5); mouse DPPIV, dipeptidyl peptidase IV (accession no. 1352312); human DPPIV, dipeptidyl peptidase IV (accession no. 1352311); *Xenopus laevis* DPPIV, dipeptidyl peptidase IV (accession no. 1621279); FAP, fibroblast activating protein (#1888316).

Note: a web page is available at http://www.fu-berlin.de/sfb366/

(Received 3 April 2000, accepted 13 June 2000)

DPPIV-isoforms [20]. Even within one species, e.g. mouse, the DPPIV/ADA interaction can be hindered [21]. Because it interacts with collagen, dipeptidyl peptidase IV belongs to the group of cell adhesion molecules (CAM) [22,23]. Binding to collagen types I and III is also mediated by the cysteine-rich domain [24].

The tertiary structure of this multifunctional protein has not been elucidated, but initial studies on its determination have been reported [25–27]. Because the 12 cysteine residues could potentially form up to six intramolecular cysteine bridges, they may be highly involved in the formation of the native DPPIV structure and therefore essential for interactions with other proteins. In this work we elucidated the influence of all 12 cysteines concerning structural and biological properties in stable expressed mutated protein.

EXPERIMENTAL PROCEDURES

Sequence alignment of rat DPPIV with homologous proteins

The sequence of rat DPPIV was compared with those of different members of the serine–protease family using nonredundant SWISSPROT Protein Sequence Database. Using the MULTALIN software [28], highest similarities were found with DPPIV from man, mouse and *Xenopus* and the human fibroblast activating protein (FAP).

Purification of DPPIV from plasma membranes

Native DPPIV from the livers of adult male Wistar rats was purified by Concavalin A and immunoaffinity chromatography as described earlier [24]. The purity of the protein preparation was determined by SDS/PAGE, and the enzymatic activity was measured in solution using the chromophoric reagent Gly-Pro4-nitroanilide-tosylate as substrate [29].

Titration of free sulfhydryl-groups

Purified DPPIV from rat liver was titrated with 5,5′-dithiobis-(2-nitrobenzoic acid) (Nbs_2) according to Pecci and co-workers [30]. Titrations were performed under native (0.1 M Tris/HCl, pH 7.8) or denaturing (6.4 M guanidine HCl, pH 6.0) conditions at 25 °C for up to 4 h. Extinction was measured at 410 nm at different times during the incubation period.

Construction of mutant DPPIV, vector construction and site-directed mutagenesis

Wild-type DPPIV *Hin*dIII–*Xho*I fragment (bp 35–2398) was cloned into the pRc/CMV expression vector (Invitrogen), and confirmed by endonuclease mapping. Each point mutation was generated using site-directed mutagenesis with synthetic oligonucleotides bearing the desired mutation (Table 1). The reactions were performed using the Stratagene Quikchange-system. Mutant C326G was generated with the Amersham Sculptor-system. Starting material for this mutant was DPPIV-wild-type *Pst*I–*Pst*I fragment (bp 737–1077) cloned into the multiple cloning site of the M13mp18-vector (Amersham).

All mutants were confirmed by sequence analysis using the Sanger method. Cloning steps were monitored by restriction endonuclease mapping and sequence analysis.

Table 1. Mutagenic oligonucleotides for site-directed mutagensis of rat-DPPIV: mismatches with the template are underlined.

Name	Mutagenic oligonucleotide
C299G	GGATCACTACTTGGGTGACGTGGCCTGGGTTTCAGAAG
C326G	CATAGTCGCCGATCGCC
C337S	CCACCCTAGTATGGAACTCTCCAACGACGC AG
C383G	GGCTACAAACACATCGGCCAGTTCCAGAAAGATAGG
C395S	GGAAACCCGAACAGGTCTCTACATTTATTACAAAAGGAGCC
C445S	CCACACAAATAAGAAGAGCCTTAGTTGTGACCTGAATCCA G
C448S	GAAGTGCCTTAGTTCTGACCTGAATCCAGAAAGATGCC
C455G	CCTGAATCCAGAAAGAGGCCAGTATTACTCGGTGTCAC
C473S	CTATCAGCTGGGATCCCGGGGCCCTG
C552S	GTATATGCAGGTCCCTCTAGTCAAAAAGCAGATGCTG
C650G	GTGGCGTGTTCAAGGGTGGAATAGCCGTG
C763S	CCATTTCCTCCAGCAGTCCTTCTCCTTACGCTAGC

Transfection of Chinese hamster ovary cells and selection of stable transfectants

Each plasmid DNA (2–4 μg) was transfected in 4×10^5 cells using the Eppendorf Multiporator and an appropriate Eppendorf protocol. Transfectants were cultured in six-well plates in α-modified Eagle's medium (MEM) containing 440 $mg \cdot L^{-1}$ L-glutamine and 10% fetal bovine serum for 2 days, then selected with 400 $mg \cdot L^{-1}$ geneticin G418. DPPIV-expressing cells were selected by flow cytometry with the FACS Vantage cell-sorter (Becton Dickinson). The stability of the transfectants varied in a range of a few days (e.g. mutant C448S) to 4 months (e.g. mutants C395S, C299G).

Flow cytometry of stable transfectants

Stable transfected cells were harvested from 10-cm culture plates with NaCl/P_i (0.05% w/v EDTA), pH 7.4 and washed twice with NaCl/P_i, pH 7.4. Cells were fixed with NaCl/P_i containing 3% (v/v) formaldehyde for 10 min at room temperature. For intracellular staining, cells were permeabilized for 5 min with 0.1% (v/v) Triton X-100 in NaCl/P_i at room temperature. For immunostaining, polyclonal antiserum against wild-type DPPIV or monoclonal antibody (mAb) 13.4 against the cysteine-rich domain of wild-type DPPIV was used at room temperature for 2 h. After intensive washing with NaCl/P_i, cells were incubated for 1 h at room temperature with fluorescein isothiocyante (FITC)-labeled rabbit anti-mouse Ig (for mAb 13.4) and goat anti-(rabbit IgG) Ig (for polyclonal antibodies) (Sigma Immunochemicals, dilution 1 : 200) and washed carefully. Cells then were analyzed using a FACScan flow cytometer (Becton Dickinson).

Determination of enzymatic activity of DPPIV

The cell pellet obtained from a 10-cm dish was solubilized with 0.15 M NaCl/10 mM Tris/1 mM $CaCl_2$ containing 1% (v/v) Triton X-100, pH 7.4 and 1 mmol protease–inhibitor mix (Sigma, P 2714) for 2 h at 4 °C. Enzymatic activity was determined as described with Gly-Pro4-nitroanilide as substrate [29]. Relative DPPIV specific activity was calculated by comparison with the activity of the same amount of protein from wild-type DPPIV and mutants. To normalize differences in the expression level, DPPIV Western blots were performed in parallel and the intensities of bands at 100 and 110 kDa

were determined with IPLABGEL software (Signal Analytics Corporation). Statistical analysis used the Student's *t*-test.

Immunoprecipitation and Western blot analysis

Harvested cells were solubilized, followed by centrifugation at 40 000 *g* for 30 min. Aliquots of the supernatant were subjected to Western blotting in different procedures.

For immunoprecipitation, the supernatant was incubated with protein A–Sepharose bound mAb 13.4, or protein A–Sepharose bound polyclonal antibodies for 12 h at 4 °C. After intensive washing, immunoprecipitates were eluted by boiling for 5 min in SDS/sample buffer. SDS/PAGE was performed according to Laemmli [31]. Separated proteins were transferred onto a nitrocellulose membrane. Immunostaining was performed with mAb 13.4 or polyclonal antibodies and visualized by chemiluminescence.

Detection of active DPPIV after blotting

Immunoprecipitates were obtained as described above and incubated with reducing or nonreducing SDS/sample buffer for 15 min at ambient temperature before loading the gel. After blotting, the membrane was treated with the modified DPPIV substrate Gly-Pro4-methoxy-β-naphtylamide, and active DPPIV was visualized by the Fast Garnet method according to Walborg *et al*. [32].

Protein cross-linking

Cells were solubilized in NaCl/P_i, pH 8.3, containing 1% v/v Triton X-100, 3 mmol EDTA and 1 mmol protease–inhibitor mix (Sigma, P 2714) at 4 °C overnight followed by centrifugation at 40 000 *g* for 30 min.

Two hundred microliters of the supernatant were mixed with 2 μL (25 mg·mL^{-1} in dimethylsulfoxide) of disuccinimidyl-suberate (DSS) and incubated for 10 min at ambient temperature. The reaction was stopped by adding 16 μL of 0.1 M Tris/HCl, pH 8.0. Mixtures were boiled with reducing sample buffer for 5 min and loaded onto a 6% gel for SDS/PAGE. Western blotting and detection was performed as described.

^{35}S-labeling of DPPIV by pulse–chase method

Pulse–chase experiments were performed as described earlier [15]. Polyclonal anti-DPPIV antiserum from rabbit was used for immunoprecipitation. Quantification of radioactivity of protein bands on a Phosphor Imager (Molecular Dynamics) was carried out with IPLABGEL-Software.

RESULTS

Sequence alignment revealed highly conserved cysteine residues in serine proteases. Sequence analysis was performed by comparing the protein sequence of rat DPPIV with the non-redundant Genbank using MULTALIN software (see Experimental procedures). Sequence similarities with different members of the serine protease family are well known [26]. Focussed on the cysteine-rich domain, the cysteine residues of DPPIV from different species and of homologous serine proteases are highly conserved (Table 2). Amino-acid positions 326, 337, 445, 448, 455, 473, 650 and 763 are occupied by cysteines in all regarded proteins. Residue 552 is also highly conserved exept for DPPIV from *Xenopus laevis*. Cysteines 299, 383 and 395 were found only in mammalian DPPIV. We presume that these highly conserved cysteines of rat DPPIV play a critical role in the structure and function of this enzyme.

Table 2. Positions of DPPIV cysteine residues, showing similarities with homologous members of the serine protease family.

Position	DPPIV rat	DPPIV mouse	DPPIV human	DPPIV *Xenopus*	FAP human
299	C	C	C	S	S
326	C	C	C	C	C
337	C	C	C	C	C
383	C	C	C	H	H
395	C	C	C	–	A
445	C	C	C	C	C
448	C	C	C	C	C
455	C	C	C	C	C
473	C	C	C	C	C
552	C	C	C	G	C
650	C	C	C	C	C
763	C	C	C	C	C

Detection of six free cysteine residues in native rat DPPIV

Titration of native rat DPPIV with an excess of Nbs_2 showed the presence of six free sulfhydryl groups after 4 h incubation. There were slight differences between the titration kinetics in nondenaturating and denaturating buffers (Fig. 1). Under denaturating conditions, the equivalent of three to four SH-groups had been titrated after 30 min, compared with 1 equivalent under nondenaturating conditions. This reaction proceeds to 2 equivalent after 2 h and leads to a total number of six SH-groups after 3 h. The same result of six SH-equivalents after 3 h is obtained under denaturating conditions.

Generation of different Cys-Gly or Cys-Ser point mutations by site-directed mutagenesis

No intermolecular cysteine bridges could be found in the homodimer of native rat DPPIV (K. Löster, personal communication).

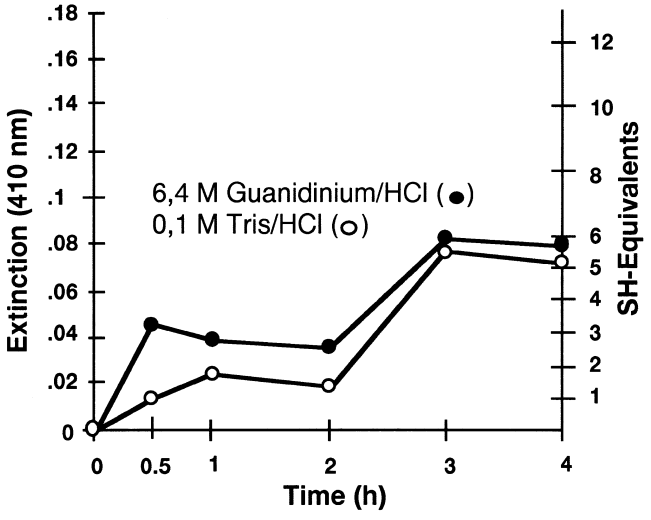

Fig. 1. Titration of native DPPIV from rat liver exhibits six free SH groups. Experiments were performed in triplicate with 5,5′-dithiobis-(2-nitrobenzoic acid) under denaturing (6.4 M guanidinine HCl) and nondenaturing (0.1 M Tris/HCl) conditions.

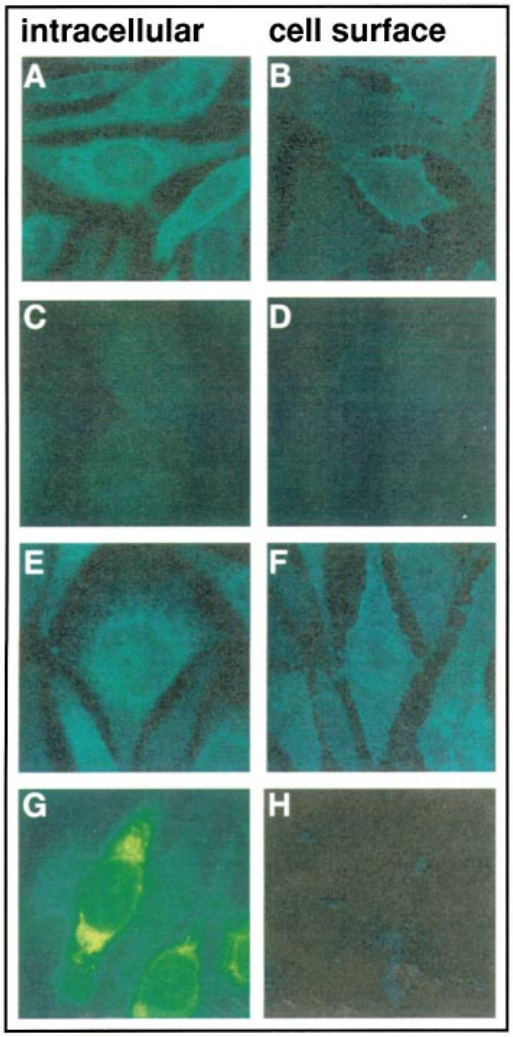

Fig. 2. Cellular localization of DPPIV in stable transfected Chinese hamster ovary (CHO) cells after immunofluorescence microscopy. DPPIV expression was detected with polyclonal antiserum. (A, B) Wild-type DPPIV; (C, D) vector-only transfectants; (E, F) C763S; (G, H) C326G.

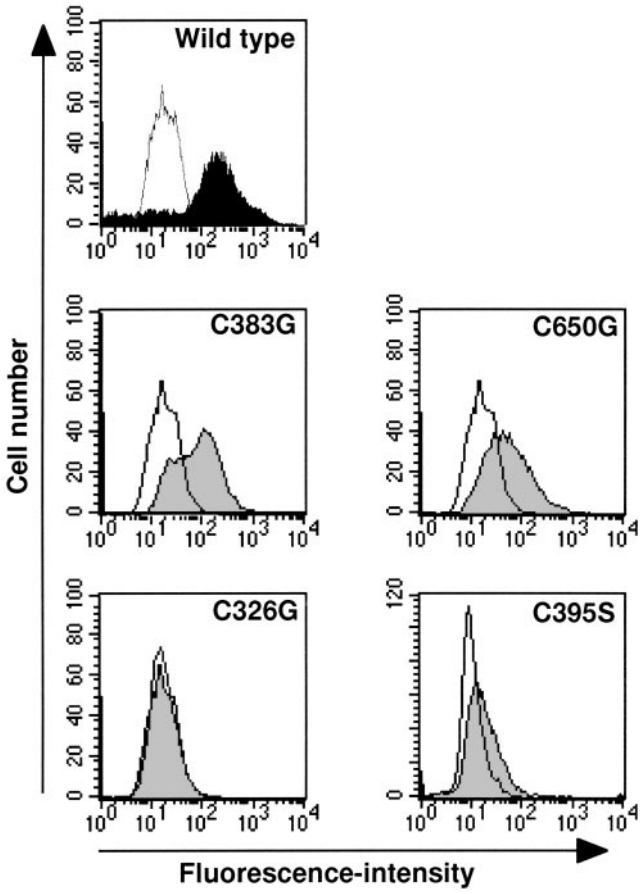

Fig. 3. Monoclonal antibody 13.4 epitope is affected in distinct cysteine mutants of DPPIV. FACS analysis of stable transfected CHO cells after intracellular staining with mAb 13.4 as first antibody. C383G and C650G: normal mAb 13.4 recognition, C326G: no recognition, C395S: reduced recognition (transfectants: hatched charts, negative-controls: clear charts).

To investigate the potential role of cysteine residues in intramolecular cystine bridge formation, we converted five of the 12 cysteine residues into glycine and seven to serine. The cysteine point mutations C299G, C326G, C337S, C383G, C395S, C445S, C448S, C455G, C473S and C552S all cover the cysteine-rich domain of DPPIV and will probably be involved in the formation of cysteine bridges. Mutations C650G and C763S are located directly in the catalytic domain of the enzyme. A potential cysteine bridge in the catalytic domain would be essential for a correct formation of this domain and therefore for enzymatic activity. The mutants were separately cloned into the eukaryotic expression vector pRc/CMV. The correct mutations were confirmed by sequencing. Generation and subcloning of the DPPIV constructs were performed as described in Experimental procedures.

Localization of wild-type and mutant DPPIV in stable transfected Chinese hamser ovary cells determined by FACS analysis

DPPIV constructs in the eukaryotic expression vector pRc/CMV were transfected into Chinese hamster ovary (CHO) cells, a fibroblast like cell-line, and grown under geniticin selection. CHO cells were chosen because of their lack of endogenous DPPIV. Stable transfectants were detected by immunofluorescence and FACS analysis and selected by cell-sorting. Wild-type DPPIV can be found on the cell surface, in the endoplasmic reticulum (ER) and the Golgi apparatus (Figs 2A,B). Mutants C299G, C383G, C395S, C455G, C473S, C552S, C650G and C763S (Figs 2E,F) exhibit the same expression pattern with a decrease of cell-surface expression in the case of mutants C455G, C473S and C552S (data not shown). Mutants C326G (Figs 2G,H), C337S and C445S and C448S can only be detected inside the cells. These experiments were performed using polyclonal anti-DPPIV serum. In contrast, mutants C326G, C337S and C455G were not detectable with the monoclonal anti-DPPIV Ig 13.4 (mAb 13.4), whose epitope is in the cysteine-rich domain of DPPIV [24]. In addition, mAb 13.4 shows a significantly weaker affinity to C395S, C445S, C448S, C473S and C552S. Figure 3 exemplifies the intracellular recognition of wild-type protein and mutants C383G, C650G, C326G and C395S by FACS-analysis after mAb 13.4 staining.

Western blot analysis of the expression pattern

Protein expression of wild-type and mutant DPPIV in CHO cells was examined by immunoprecipitation and Western blot

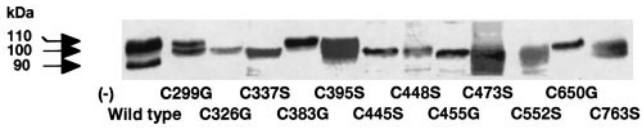

Fig. 4. Western blot analysis of DPPIV after reductive 6% SDS/PAGE. 110-kDa protein bands represent mature, 100 kDa bands represent immature and bands 90 kDa represent the degraded form of monomeric protein. Mock-transfected cells were used as negative control (–).

analysis (Fig. 4). Under reducing and denaturing conditions, glycosylated wild-type DPPIV exhibits an expression pattern with a major protein band of ≈ 110 kDa, and a weaker band at 100 kDa. The 110-kDa band represents mature protein with N-linked complex and hybrid oligosaccharides. Immature protein with N-glycans of high-mannose-type appears at 100 kDa [15]. The 90-kDa band represents degraded DPPIV. Expression patterns of the cysteine mutants can be divided in two groups:

(a) Completely processed mutants able to form the mature wild-type-like 110-kDa protein. This pattern is expressed by C299G, C383G, C395S, C650G and C763S.

(b) Mutants C326G, C337S, C445S, C448S, C455G, C473S and C552S, which do not show a band with a molecular mass > 100 kDa and therefore are not processed properly.

Half-life determination with radiolabeled mutant DPPIV

The immunofluorescence and Western blotting results show different influences of individual cysteine residues on trafficking, processing and stability of DPPIV. Mutants that do not form the mature 110-kDa form are not expressed on the cell surface, so that their trafficking is different from that of wild-type DPPIV. Radiolabeling of DPPIV-transfected CHO cells with [^{35}S]methionine/cysteine, followed by autoradiography of the immunoprecipitated and blotted enzyme, revealed major differences in the half-life ($t_{1/2}$) of cysteine mutants. The half-life, calculated using IPLABGEL software from the intensities of the 100-kDa and 110-kDa forms, is ≈ 55 h in case of wild-type DPPIV. Mutants C299G, C395S and C650G show similar stabilities. Cysteine mutants C326G, C337S, C383G, C448S and C763S show significantly lower stability with $t_{1/2}$ values between 12 and 30 h. The half-life of mutants C445S, C455G, C473S and C552S is decreased dramatically to < 10 h. Figure 5A shows wild-type DPPIV, C383G, C337S and C455G as examples.

Wild-type and mutant DPPIV show different processing kinetics

Determination of half-life periods reveals a strong influence of defined cysteine residues on protein stability and degradation. There are not only quantitative changes in protein stability but also significant differences in the kinetics of processing and degradation of newly synthesized mutant DPPIV. Kinetics were determined by consideration of all three DPPIV forms of 90, 100 and 110 kDa from pulse–chase experiments. For all 12 mutants, the ratio of the three forms was calculated at different times from 0 to 48 h with IPLABGEL software. The total amount of protein (i.e. the intensity of the respective bands on the autoradiograph) is set as 100% for each time-point (Fig. 5B). After pulse-labeling, wild-type DPPIV processing starts at 0 h with almost equal amounts of nonprocessed 100 kDa (55%) and mature 110-kDa protein (45%). At 1 h chase, the ratio of 100 : 110 kDa has changed to 30 : 70, whereas the immature 100-kDa protein disappears after 5 h. At this time, 95% of wild-type DPPIV has been processed properly. Degradation of wild-type protein could not be detected earlier than 2.5 h, and after 48 h the ratio of mature to degraded protein had reached 65 : 35. Mutants C299G, C383G, C395S, C650G and C763S show similar kinetics, as illustrated for C383G. Cysteine mutants C326G, C337S, C445S, C448S and C473S show a second processing kinetic, exemplified by C337S. The immature 100-kDa form of these mutants is processed significantly more slowly; thus in the case of C337S mature protein first appears after 5 h of processing. In addition, mature 110-kDa protein shows only weak stability, and degraded DPPIV appears a short time after the 110-kDa form. After 48 h the ratio between 110, 100 and 90-kDa forms is 40 : 30 : 30. The processing pattern

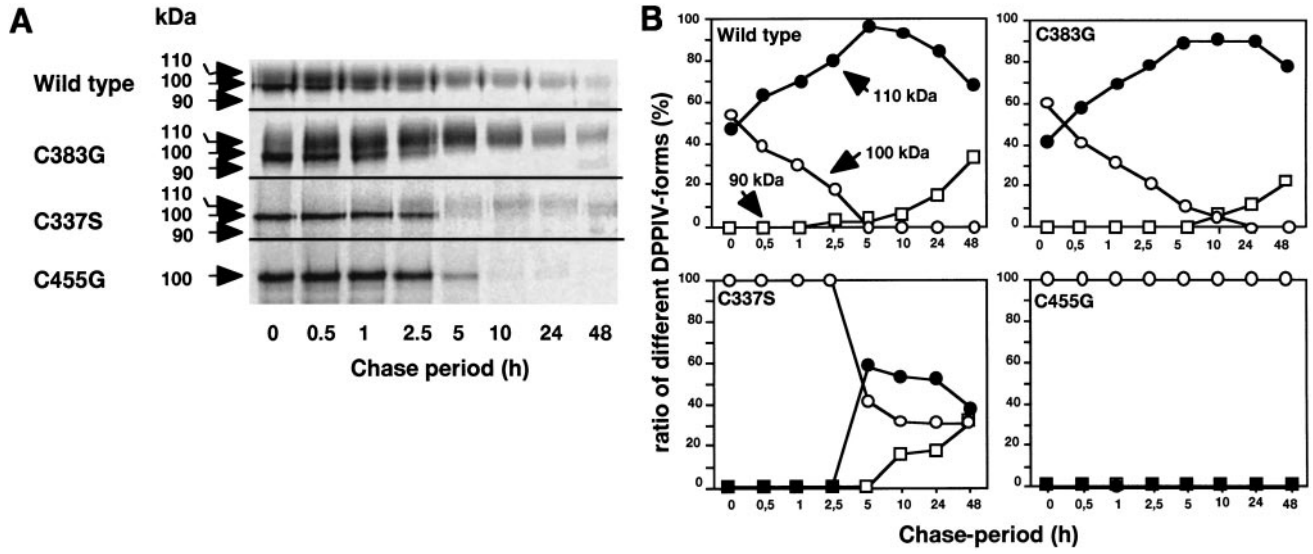

Fig. 5. Half-life and protein-processing kinetics of DPPIV. (A) Autoradiographs of pulse–chase ^{35}S-labeled and immunoprecipitated DPPIV (mutants). Protein obtained from equal cell numbers was subjected to reducing SDS/PAGE and Western blotting prior to autoradiography. (B) Three different processing kinetics computed from autoradiographs.

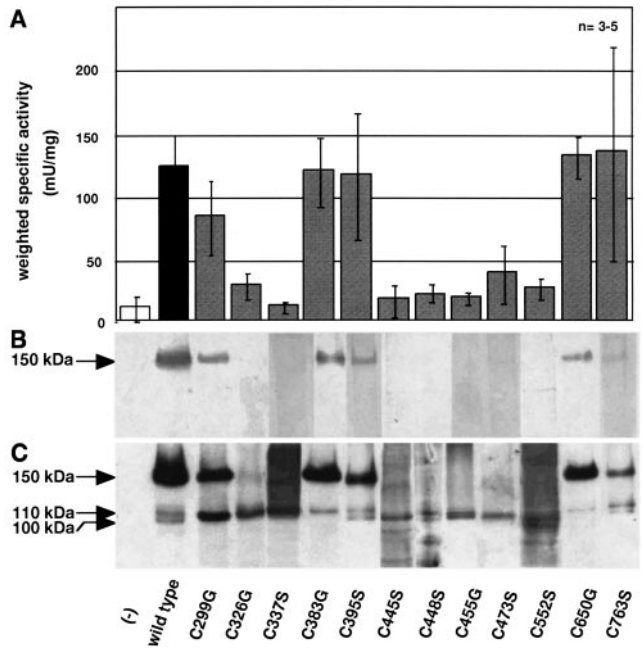

Fig. 6. Normalized specific enzymatic activity from solubilized transfectants (A), DPPIV-bands showing specific enzymatic activity in a Fast garnet blot after nonreductive 6% SDS/PAGE and Western blotting (B) and Western blot analysis of immunoprecipitated DPPIV after nonreductive 6% SDS/PAGE (C). 150 kDa represents the active dimeric form, 110 kDa represents the mature monomeric form, and 100 kDa represents the immature form of monomeric DPPIV.

of mutant C455G is also shown in Fig. 5. This kinetic, also found at mutant C552S, is totally different because only immature 100-kDa protein is expressed over the whole chase period. Neither mature 110-kDa protein nor the degradation product of 90 kDa could be detected.

Enzymatic activity of mutant DPPIV depends on correct protein folding

Relative enzymatic activity of wild-type DPPIV was compared with the activity of cysteine mutant proteins. To eliminate differences in the strength of expression, equal amounts of immunoprecipitated protein were used for activity determination. All assays were repeated three to five times with different cell lysates of stable transfectants (Fig. 6A). Taking wild-type DPPIV activity set as 100%, mutants C383G, C395S, C650G and C763S exhibit comparable activity. Untransfected CHO cells show low endogenous activity. In the case of cysteine mutants C326G, C473S and C552S, peptidase activity is reduced dramatically, whereas C337S, C445S, C448S and C455G do not exhibit significant activity.

In view of the heterogeneous expression pattern of the different mutants, we determined the enzymatic active expression products by the Fast garnet procedure as described in Experimental procedures. Under nonreducing conditions, all mutants with strong enzymatic activity (C299G, C383G, C395S, C650G, C763S) show an active band at 150 kDa, similar to wild-type DPPIV (Fig. 6B). No active band was detected for the cysteine mutants with low or insignificant enzymatic activity. It has to be mentioned, that this procedure is less sensitive than activity measurements in cell lysates. A standard Western blot under the same conditions shows the expression of all mutant proteins and shows that enzymatic activity depends on the existence of a band with an apparent molecular mass of 150 kDa (Fig. 6C).

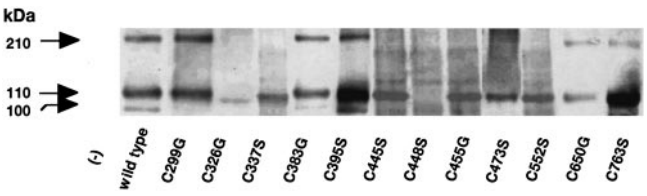

Fig. 7. Western blot analysis of DSS cross-linked DPPIV after reductive 6% SDS/PAGE. 210 kDa bands represent dimeric peptidase in addition to the monomeric forms at 100 and 110 kDa. Reaction of distinct mutants (particularly C448S) with polyclonal antiserum was decreased. Not cross-linked controls show normal expression (data not shown).

Formation of DPPIV homodimers

To exhibit a potential role of the mutated cysteines in the formation of the DPPIV homodimer, detergent-solubilized DPPIV mutants were incubated with the homobifunctional and noncleavable cross-linker DSS (Fig. 7). DSS cross-linked wild-type DPPIV shows an expression pattern with the 110-kDa monomeric and 210 kDa homodimeric form. Mutants C299G, C383G, C395S, C650G and C763S are also capable of dimer formation. From these results we conclude that in the case of C326G, C337S, C445S, C448S, C455G, C473S and C552S certain disulfide bridges have been destroyed by elimination of one cysteine residue. The removal of a single disulfide bridge might lead to a conformational change in the corresponding cysteine-rich domain of DPPIV which obviously has importance for dimer formation. In contrast, replacement of a cysteine residue with serine or glycine might be sufficient to prevent dimerization.

DISCUSSION

In this study the influence of all 12 cysteine residues on the structure and function of the multifunctional membrane glycoprotein dipeptidylpeptidase IV/CD26 was investigated. The primary structure of rat peptidase is very similar to those of other members of the serine-protease family, e.g. human, mouse and *Xenopus*-DPPIV and FAP [18]. These similarities are reflected by the eight highly conserved cysteine residues.

To elucidate which residues are involved in bridge formation and therefore relevant for protein structure we generated 12 different point mutations using site-directed mutagenesis. In each mutant, one of the 12 cysteine residues was mutated either to glycine (mutants C299G, C326G, C383G, C455G and C650G) or to the structural homolog serine (mutants C337S, C395S, C445S, C448S, C473S, C552S and C763S). Investigations with stable transfected CHO cells revealed that these cysteine mutations induce different effects concerning the expression pattern and intracellular translocation as well as the *in vitro* proteolytic activity of the protein.

Mutants C299G, C383G, C395S, C650G and C763S show wild-type like intracellular and cell-surface expression. In the case of mutants C337S, C455G, C473S and C552S, surface expression is decreased significantly, whereas C326G, C445S and C448S could be detected only intracellularly. FACS analysis of transfected cells shows that mutation of cysteines 326, 337 or 455 totally inhibits the recognition of the mutated protein by mAb 13.4. This mAb has its epitope within the cysteine-rich region of DPPIV [24]. These mutations obviously

lead to severe structural changes in the cysteine-rich domain of DPPIV. Detection of mutants C395S, C445S, C448S, C473S and C552S is decreased significantly. The mAb 13.4 epitope is less affected in the latter mutants.

The formation of cystine bridges occurs cotranslationally in the ER and has an important impact on correct protein folding [33]. This folding process is supported by chaperones like HSP 40, 60 and 70. In the case of glycoproteins like DPPIV, calnexin and calreticulin are required [34]. Incorrect folding leads to retention in the ER and the misfolded proteins are degraded, as shown with N-glycan defective DPPIV mutants [15]. The influence of this quality control mechanism results in a dramatic change in the expression patterns of mutants C326G, C337S, C445S, C448S, C455G, C473S and C552S but not of C299G, C383G, C395S, C650G and C763S. Mature monomeric DPPIV at 110 kDa could not be detected in the first group, but a 100-kDa form was present, which represents immature protein with oligosaccharides of high-mannose type. This immature form of newly synthesized protein exists predominantly in the ER. N-glycan processing from high-mannose to complex and hybrid type occurs in the Golgi apparatus and leads to mature DPPIV with a molecular mass of 110 kDa. In consequence, intracellular trafficking of the peptidase is decreased or inhibited totally by the mutation of cysteine residues C326, C337, C445, C448, C455, C473 or C552. Significant alterations in processing kinetics and drastically reduced half-lives of these mutants, compared with the wild-type protein revealed further influences of these cysteine residues on the structure, stability and trafficking of DPPIV. In addition, mutants C455G and C552S showed very similar half-lives and processing kinetics. These residues might be involved in the formation of the same disulfide bridge. Determination of the dimeric state of mutants C326G, C337S, C445S, C448S, C455G, C473S and C552S revealed that they are significantly disturbed structurally. In general, plasma-membrane glycoproteins tend to be oligomers with the oligomerization occurring in the ER [35,36]. Studies have shown that dimerization of DPPIV also occurs in the ER and has to be seen as a prerequisite for transport to the Golgi apparatus and beyond [10], although Jascur *et al*. [11] favor the late Golgi compartment as the site of dimerization. Our processing kinetics provided evidence that only cysteine mutants capable of forming wild-type-like glycosylation pattern will dimerize. The extent of N-glycan processing is not decisive for dimerization because all N-glycans consist of high-mannose structures in the ER. We conclude that structural alterations of newly synthesized DPPIV caused by the cysteine mutations C326G, C337S, C445S, C448S, C455G, C473S and C552S are the reason for nondimerization. Furthermore, the enzymatic activity of DPPIV/CD26 is abolished in mutants C337S, C445S, C448S, C455G and drastically reduced in C326G, C473S and C552S. In contrast, mutants C650G and C763S, which are mutated in the catalytic domain, show no effect. These results indicate that there is no bridge formation by cysteines C763 and C650 in the active site. The strong inhibitory effect of mutation of distant cysteine residues suggests tight structural interactions between the three extracellular domains.

These findings fit well with the preliminary β-propeller structure of the cysteine-rich domain of human DPPIV predicted by Abbott and co-workers [27]. Following this model, cysteines C326/C337, C383/C395, C445/C448 and C455/C473 are located pairwise on different propeller blades. It can be speculated about propeller structures stabilized by intrablade disulfide bonds. As DPPIV belongs to a special subfamily of serine proteases, the prolyl oligopepidases, the α/β-hydrolase fold has been predicted for its catalytic domain [26,37,38]. This model includes no indications for a disulfide bond within the C-terminal domain which is in accordance with the wild-type like characteristics of mutants C650G and C763S.

Purified wild-type DPPIV was used for SH titration experiments to determine the number of reduced sulfhydryl groups. Six of the 12 SH groups were found to be free under denaturing and nondenaturing conditions. We conclude that all free cysteines of DPPIV are accessible to Nbs_2 in the native conformation of the enzyme. Two cysteines react faster under denaturing conditions, so they might be located near the surface in the native conformation of DPPIV. From these results we conclude that there are three intramolecular disulfide bridges which is in accordance to the preceding biochemical analysis.

In conclusion, our results from sequence analysis, as well as the experiments on the structure–function relationships of DPPIV/CD26 revealed the existence of six reduced cysteine residues and three intramolecular disulfide bridges. Cysteines C299, C383, C395, C650 and C763 are obviously not involved in bridge formation. Residues C326, C337, C445, C448, C455, C473 and C552 are, to different extents, essential for the tertiary structure and biological properties of the enzyme. The disulfide bridges will be located with greater certainty by forthcoming peptide mapping experiments.

ACKNOWLEDGEMENTS

This work was supported by a grant from the Deutsche Forschungsgemeinschaft, Bonn (Sonderforschungsbereich 366), the Sonnenfeld-Stiftung and the Fonds der Chemischen Industrie, Frankfurt/Main. We are grateful to Dr G. Krause (Forschungsinstitut für Molekulare Pharmakologie, Berlin) for scientific discussions.

REFERENCES

1. Hopsu-Havu, V.K. & Glenner, G.G. (1966) A new dipeptide naphthylamidase hydrolyzing glycyl-prolyl-beta-naphthylamide. *Histochemie* **7**, 197–201.
2. Hopsu-Havu, V.K. & Makinen, K.K. (1967) The hydrolysis of amino acid naphthylamides by the human seminal aminopeptidase. *Arch. Klin. Exp. Dermatol.* **228**, 316–326.
3. Morimoto, C. & Schlossman, S.F. (1998) The structure and function of CD26 in the T-cell immune response. *Immunol. Rev.* **161**, 55–70.
4. von Bonin, A., Steeg, C., Mittrucker, H.W. & Fleischer, B. (1997) The T-cell receptor associated zeta-chain is required but not sufficient for CD26 (dipeptidylpeptidase IV) mediated signaling. *Immunol. Lett.* **55**, 179–182.
5. Kahne, T., Lendeckel, U., Wrenger, S., Neubert, K., Ansörge, S. & Reinhold, D. (1999) Dipeptidyl peptidase IV: a cell surface peptidase involved in regulating T cell growth (review). *Int. J. Mol. Med.* **4**, 3–15.
6. Kyouden, T., Himeno, M., Ishikawa, T., Ohsumi, Y. & Kato, K. (1992) Purification and characterization of dipeptidyl peptidase IV in rat liver lysosomal membranes. *J Biochem. Tokyo* **111**, 770–777.
7. Hutchinson, D.R., Halliwell, R.P., Lockhart, J.D. & Parke, D.V. (1981) Glycylprolyl-*p*-nitroanilidase in hepatobiliary disease. *Clin. Chim. Acta* **109**, 83–89.
8. Vlasak, R., Vilas, U., Strobl, B. & Kreil, G. (1997) cDNA cloning and expression of secreted *Xenopus laevis* dipeptidyl. *Eur. J. Biochem.* **247**, 107–113.
9. Elovson, J. (1980) Biogenesis of plasma membrane glycoproteins. Tracer kinetic study of two rat liver plasma membrane glycoproteins *in vivo*. *J. Biol. Chem.* **255**, 5816–5825.
10. Danielsen, E.M. (1994) Dimeric assembly of enterocyte brush border enzymes. *Biochemistry* **33**, 1599–1605.
11. Jascur, T., Matter, K. & Hauri, H.P. (1991) Oligomerization

and intracellular protein transport: dimerization of intestinal dipeptidylpeptidase IV occurs in the Golgi apparatus. *Biochemistry* **30**, 1908–1915.
12. Ogata, S., Misumi, Y. & Ikehara, Y. (1989) Primary structure of rat liver dipeptidyl peptidase IV deduced from its cDNA and identification of the NH_2-terminal signal sequence as the membrane-anchoring domain. *J. Biol. Chem.* **264**, 3596–3601.
13. Marguet, D., Bernard, A.M., Vivier, I., Darmoul, D., Naquet, P. & Pierres, M. (1992) cDNA cloning for mouse thymocyte-activating molecule. A multifunctional ecto-dipeptidyl peptidase IV (CD26) included in a subgroup of serine proteases. *J. Biol. Chem.* **267**, 2200–2208.
14. Misumi, Y., Hayashi, Y., Arakawa, F. & Ikehara, Y. (1992) Molecular cloning and sequence analysis of human dipeptidyl peptidase IV, a serine proteinase on the cell surface. *Biochim. Biophys. Acta* **1131**, 333–336.
15. Fan, H., Meng, W., Kilian, C., Grams, S. & Reutter, W. (1997) Domain-specific N-glycosylation of the membrane glycoprotein dipeptidyl-peptidase IV (CD26) influences its subcellular trafficking, biological stability, enzyme activity and protein folding. *Eur. J. Biochem.* **246**, 243–251.
16. Ogata, S., Misumi, Y., Tsuji, E., Takami, N., Oda, K. & Ikehara, Y. (1992) Identification of the active site residues in dipeptidyl peptidase IV by affinity labeling and site-directed mutagenesis. *Biochemistry* **31**, 2582–2587.
17. Bermpohl, F., Löster, K., Reutter, W. & Baum, O. (1998) Rat dipeptidyl peptidase IV (DPP IV) exhibits endopeptidase activity with specificity for denatured fibrillar collagens. *FEBS Lett.* **428**, 152–156.
18. Augustyns, K., Bal, G., Thonus, G., Belyaev, A., Zhang, X.M., Bollaert, W., Lambeir, A.M., Durinx, C., Goossens, F. & Haemers, A. (1999) The unique properties of dipeptidyl-peptidase IV (DPP IV/CD26) and the therapeutic potential of DPP IV inhibitors. *Curr. Med. Chem.* **6**, 311–327.
19. Buhling, F., Junker, U., Reinhold, D., Neubert, K., Jäger, L. & Ansörge, S. (1995) Functional role of CD26 on human B lymphocytes. *Immunol. Lett.* **45**, 47–51.
20. Dong, R.P., Tachibana, K., Hegen, M., Munakata, Y., Cho, D., Schlossman, S.F. & Morimoto, C. (1997) Determination of adenosine deaminase binding domain on CD26 and its immunoregulatory effect on T cell activation. *J. Immunol.* **159**, 6070–6076.
21. Dong, R.P., Kameoka, J., Hegen, M., Tanaka, T., Xu, Y., Schlossman, S.F. & Morimoto, C. (1996) Characterization of adenosine deaminase binding to human CD26 on T cells and its biologic role in immune response. *J. Immunol.* **156**, 1349–1355.
22. Hanski, C., Huhle, T. & Reutter, W. (1985) Involvement of plasma membrane dipeptidyl peptidase IV in fibronectin-mediated adhesion of cells on collagen. *Biol. Chem. Hoppe-Seyler* **366**, 1169–1176.
23. Hanski, C., Huhle, T., Gossrau, R. & Reutter, W. (1988) Direct evidence for the binding of rat liver DPP IV to collagen *in vitro*. *Exp. Cell Res.* **178**, 64–72.
24. Löster, K., Zeilinger, K., Schuppan, D. & Reutter, W. (1995) The cysteine-rich region of dipeptidyl peptidase IV (CD 26) is the collagen-binding site. *Biochem. Biophys. Res. Commun.* **217**, 341–348.
25. Lambeir, A.M., Diaz Pereira, J.F., Chacon, P., Vermeulen, G., Heremans, K., Devreese, B., Van Beeumen, J., De Meester, I. & Scharpé, S. (1997) A prediction of DPP IV/CD26 domain structure from a physico-chemical investigation of dipeptidyl peptidase IV (CD26) from human seminal plasma. *Biochim. Biophys. Acta* **1340**, 215–226.
26. Goossens, F., De Meester, I., Vanhoof, G., Hendriks, D., Vriend, G. & Scharpé, S. (1995) The purification, characterization and analysis of primary and secondary-structure of prolyl oligopeptidase from human lymphocytes. Evidence that the enzyme belongs to the alpha/beta hydrolase fold family. *Eur. J. Biochem.* **233**, 432–441.
27. Abbott, C.A., McCaughan, G.W., Levy, M.T., Church, W.B. & Gorrell, M.D. (1999) Binding to human dipeptidyl peptidase IV by adenosine deaminase and antibodies that inhibit ligand binding involves overlapping, discontinuous sites on a predicted beta propeller domain. *Eur J Biochem.* **266**, 798–810.
28. Corpet, F. (1988) Multiple sequence alignment with hierarchical clustering. *Nucleic Acids Res.* **16**, 10881–10890.
29. Nagatsu, T., Hino, M., Fuyamada, H., Hayakawa, T. & Sakakibara, S. (1976) New chromogenic substrates for X-prolyl dipeptidyl-amino-peptidase. *Anal Biochem.* **74**, 466–476.
30. Pecci, L., Cannella, C., Pensa, B., Costa, M. & Cavallini, D. (1980) Cyanylation of rhodanese by 2-nitro-5-thiocyanobenzoic acid. *Biochim. Biophys. Acta* **623**, 348–353.
31. Laemmli, U.K. (1970) Cleavage of structural proteins during the assembly of the head of bacteriophage T4. *Nature* **227**, 680–685.
32. Walborg, E.F. Jr, Tsuchida, S., Weeden, D.S., Thomas, M.W., Barrick, A., McEntire, K.D., Allison, J.P. & Hixson, D.C. (1985) Identification of dipeptidyl peptidase IV as a protein shared by the plasma membrane of hepatocytes and liver biomatrix. *Exp. Cell. Res.* **158**, 509–518.
33. Reddy, P.S. & Corley, R.B. (1998) Assembly, sorting, and exit of oligomeric proteins from the endoplasmic reticulum. *Bioessays* **20**, 546–554.
34. Michalak, M., Mariani, P. & Opas, M. (1998) Calreticulin, a multifunctional Ca^{2+} binding chaperone of the endoplasmic reticulum. *Biochem. Cell Biol.* **76**, 779–785.
35. Copeland, C.S., Zimmer, K.P., Wagner, K.R., Healey, G.A., Mellman, I. & Helenius, A. (1988) Folding, trimerization, and transport are sequential events in the biogenesis of influenza virus hemagglutinin. *Cell* **53**, 197–209.
36. Hurtley, S.M., Bole, D.G., Hoover-Litty, H., Helenius, A. & Copeland, C.S. (1989) Interactions of misfolded influenza virus hemagglutinin with binding protein (BiP). *J. Cell Biol.* **108**, 2117–2126.
37. Abbott, C.A., Baker, E., Sutherland, G.R. & McCaughan, G.W. (1994) Genomic organization, exact localization, and tissue expression of the human CD26 (dipeptidyl peptidase IV) gene. *Immunogenetics* **40**, 331–338.
38. Fulop, V., Bocskei, Z. & Polgár, L. (1998) Prolyl oligopeptidase: an unusual beta-propeller domain regulates proteolysis. *Cell* **94**, 161–170.